HHS Public Access

Author manuscript

Nat Protoc. Author manuscript; available in PMC 2018 March 18.

Published in final edited form as:

Nat Protoc. 2017 February ; 12(2): 355–371. doi:10.1038/nprot.2016.172.

An integrated dispersion preparation, characterization and *in vitro* dosimetry methodology for engineered nanomaterials

Glen M. DeLoid[1], **Joel M. Cohen**[1], **Georgios Pyrgiotakis**[1], and **Philip Demokritou**[1,*]

[1]Center for Nanotechnology and Nanotoxicology, HSPH-NIEHS Nanosafety Research Center, Department of Environmental Health, Harvard School of Public Health, 655 Huntington Ave Boston, MA 02115

Summary

Evidence continues to grow of the importance of *in vitro* and *in vivo* dosimetry in the hazard assessment and ranking of engineered nanomaterials (ENMs). Accurate dose metrics are particularly important for *in vitro* cellular screening to assess the potential health risks or bioactivity of ENMs. In order to ensure meaningful and reproducible quantification of *in vitro* dose, with consistent measurement and reporting between laboratories, it is necessary to adopt standardized and integrated methodologies for 1) generation of stable ENM suspensions in cell culture media, 2) colloidal characterization of suspended ENMs, particularly properties that determine particle kinetics in an *in vitro* system (size distribution and formed agglomerate effective density), and 3) robust numerical fate and transport modeling for accurate determination of ENM dose delivered to cells over the course of the *in vitro* exposure. Here we present such an integrated comprehensive protocol based on such a methodology for *in vitro* dosimetry, including detailed standardized procedures for each of these three critical steps. The entire protocol requires approximately 6-12 hours to complete.

Introduction

The unique physicochemical properties of ENMs are being exploited for use in a growing variety of commercial nano-enabled products (NEPs), including electronics, cosmetics, and structural materials, as well as a wide variety of products for antimicrobial, agricultural medical therapeutic and diagnostic applications[1–8]. The rapid proliferation and commercialization of these ENMs and associated NEPs poses a potential risk of both occupational and consumer exposures to materials for which toxicological data is extremely limited[9–17]. Moreover, the high degree of variability in physicochemical properties such as composition, size, morphology, surface topology, chemistry and modifications, crystallinity, and impurity content among these ENMs presents a significant challenge to the nanotoxicology field[18–22]. In addition, human exposure is not limited to pristine ENMs, but

*corresponding author: Philip Demokritou, pdemokri@hsph.harvard.edu, Phone: 617 432 3481.

Author Contributions: Glen DeLoid: co-wrote manuscript.
Joel Cohen: co-write manuscript.
Georgios Pyrgiotakis: co-write manuscript
Philip Demokritou: oversaw manuscript preparation and co-wrote manuscript.

Competing Financial Interests: None of the authors have any competing financial interests in the work described in this manuscript.

also includes a wide variety of particles released from NEPs across their life cycle, including at the consumer use and disposal stages[6,23,24]. Indeed, the potential for exposure from such life cycle particulate matter (LCPM) may exceed that of pristine ENMs[23]. To complicate the matter further, the physicochemical properties and toxicological profiles of LCPM may differ greatly from those of the corresponding pristine ENMs [14,25–31].

To address the vast and growing number and variety of ENMs entering the market, there is great need for fast, inexpensive and *in vivo*-validated high-throughput screening strategies based on *in vitro* cellular assays. However, *in vitro* testing results between different labs often contradict one another, and even greater disparity is observed between *in vitro* and *in vivo* results[19,20,32]. Much of this *in vitro* vs. *in vivo* disparity can be explained by the failure of simple cellular systems (which often employ immortal, i.e. highly abnormal, cell lines) to adequately recapitulate the complex milieu of a mammalian organism. However, it is likely that mismatch of *in vitro* and *in vivo* doses, due to inadequate ENM characterization, and particularly failure to adequately account for fate and transport of ENMs *in vitro*, is a significant contributor to these disparities[33–38].

In a typical *in vitro* cellular assay, ENMs are dispersed in cell culture media, and the resulting suspension is dispensed onto adherent cells in multi-well cell culture plates. Cellular responses are measured following incubation (typically 24 hours) over a range of doses to establish a dose-response relationship. The doses most often used to define these relationships are either total administered mass, surface area or number of particles, or the per volume concentration of mass, surface area or particles in the initial administered suspension. This *in vitro* hazard and bioactivity assessment approach has been widely and successfully used for industrial and environmental chemicals, as well as for drug candidates[39,40]. However, because ENMs in suspension are subject to ENM- and media-specific physicochemical transformations that affect their fate and transport, and thus the dose delivered to cells as a function of exposure time[33,36,37,41,42], it is not suitable for assessment of colloidal suspensions of ENMs.

When ENMs are suspended in cell culture media or physiological fluids they may form agglomerates consisting of multiple protein-coated primary particles and trapped intra-agglomerate fluid. The extent and kinetics of protein corona and agglomerate formation, and the size-distribution and stability of agglomerates is largely determined by the intrinsic properties of the primary ENM particles (i.e., composition, size, shape, surface chemistry), and the extrinsic properties of the fluid (i.e., ionic strength, pH, protein and other biomolecular types and content)[42,43].The degree of agglomeration and the stability of the resulting size distributions are also highly-dependent upon the methods used to disperse the ENMs in the liquid[33].These transformations have critically important effects on nano-biointeractions between suspended ENMs and cells. Agglomeration reduces the total number of particles as well as the total surface area of the suspended ENM available for interaction with cells. Indeed, cellular toxicity studies have demonstrated that agglomerated nanoparticles exert substantially different biological effects compared to those exerted by well-dispersed nanoparticles of the same material[44,45].

Agglomeration also determines the key properties that determine fate and transport of particles in suspension, namely size and effective density[36,37]. The agglomeration state of suspended ENMs can range from no agglomeration at all, with suspended forms having diameters on the same order as the primary particles, to formation of large micron-sized agglomerates containing hundreds or thousands of primary particles. Because the sedimentation rate of a particle in suspension is proportional to the square of its diameter, a 10 fold difference in size results in a 100 fold difference in sedimentation rate, and roughly the same fold difference in delivered *in vitro* dose[37]. The other key determinant of transport is effective density. Because agglomerates can contain relatively large amounts of media, the effective density of suspended ENMs can be much less than the density of the primary particle material, and is often closer to the density of the media[36]. Because the sedimentation rate is directly proportional to the difference between the media and the agglomerate effective density, this can also have a large effect on the dose delivered to cells over time. It was recently demonstrated that buoyant ENMs present a special case and challenge for characterization and dosimetric analysis[46]. If the raw material density is lower than the media density, as in the case of some conjugated polymers, nanobubbles and liposomes used in nanomedicine and food applications[47–50], the agglomerates do not settle, but instead rise or float away from cells over time, making the dose response relationship impossible to determine. We have recently demonstrated that in a standard cell culture system buoyant polypropylene ENMs have no effect on cells, whereas in an inverted cell culture system, in which cells are oriented above the ENM suspension, the same ENMs produced dose-dependent increases in cytotoxicity and reactive oxygen species generation[46].

Dosimetry can impact interpretation of *in vitro* hazard ranking results. *In vitro* nanotoxicology is comparative in nature, often relying on previously-studied nanomaterials as controls to provide hazard rankings among large panels of ENMs. However studies often fail to sufficiently characterize colloidal properties of suspended materials or to account for effects of these properties on fate and transport and the exposure dose delivered to cells. The critical role of dosimetry in interpretation of *in vitro* nanotoxicology studies was highlighted in the seminal work of Wittmaack, who reported the formation and rapid settling and accumulation of micron-sized agglomerates of suspended nanostructured powders[51]. Importantly, Wittmaack pointed out that the resulting exceedingly high exposure doses could cause physical overload effects from overlying or internalized ENMs that could be misinterpreted as toxicity. Additional studies by Wittmaack reported significant correlation between *in vitro* toxicity of SiO_2 nanoparticles and the areal density of nanoparticle mass delivered to cells over the exposure duration, further emphasizing the importance of particle kinetics in interpretation of biological responses[52].Thus, an ENM that forms large and dense, and thus rapidly sedimenting agglomerates that quickly concentrate around cells, may be reported as more toxic than one that forms smaller and less dense, and thus slower-settling agglomerates, even though the latter material might well be more toxic than the former at equivalent delivered doses[53]. Recent studies report the impact of agglomerate properties on the time required for ENM delivery to cells *in vitro*[37,54], and demonstrate the subsequent impacts of dosimetry on hazard ranking of large panels of low-aspect ratio ENMs[53].

Moreover, cell uptake and translocation *in vitro* is strongly dependent upon ENM characteristics, composition and protein content of the media and the dose delivered to cells [55,56].Thus methods for reproducibly generating ENM suspensions, and accurate ENM- and media-specific characterization and dosimetry *in vitro* are essential for predicting uptake and translocation biokinetics and biological effects *in vitro*. More importantly, doses used for *in vitro* testing should be matched with *in vivo* exposure doses, which in turn should be based upon realistic potential human exposures [34,35,39]. Until recently this was rarely done, in part because the tools necessary to correctly match *in vivo* and *in vitro* exposures have not been available. However, with accurate *in vitro* and *in vivo* computational dosimetry modeling now available it is possible to bring *in vitro* cellular and *in vivo* animal exposures into alignment. For example, delivered doses for *in vivo* particle inhalation exposures can be quantified using the multiple-path particle dosimetry model (MPPD)[57]. The MPPD provides, for a given human or animal model (lung/airway anatomy and geometry, breathing parameters), ENM aerosol characteristics, and exposure time, an estimate of the ENM mass deposited per unit area of the lung, and is the gold standard for dosimetry in animal studies of ENM inhalation exposures[34,58,59]. The *in vivo* deposited mass per unit lung area obtained from MPPD can then be used as a target deposited mass per area for *in vitro* experiments, and the corresponding initial administered *in vitro* ENM concentrations needed to obtain that target delivered dose can be determined using computational modeling approaches such as the ISDD-VCM or DG model[14,37,54,60].

Thus, In addition to errors in hazard ranking, the failure to adequately account for fate and transport likely contributes to the inconsistent results within and especially between laboratories, to skewed relationships between toxicological outcomes and physicochemical properties, and to conflicting findings between *in vitro* and *in vivo* experiments. For these reasons, development of an integrated, validated dosimetry methodology has become a high priority in *in vitro* nanotoxicology.

Recently, integrated, hybrid *in vitro* dosimetric platforms have been developed to address this important issue. Such integrated platforms include the preparation and proper characterization of ENM suspensions and the use of advanced numerical fate and transport methods to estimate the delivered dose metrics[37,54]. Here we provide a detailed protocol for such a methodology, which if adopted could ensure consistent test ENM suspensions for *in vitro* toxicological testing across laboratories, and accurate calculation of dose metrics as a function of exposure time in an *in vitro* culture system.

Development of the protocol based on the integrated *in vitro* dosimetry methodology

We present here a multi-step *in vitro* dosimetric methodology that enables nanotoxicologists to quantify delivered dose metrics as a function of time[54]. This methodology consists of three interconnected parts: 1) ENM dispersion preparation; 2) ENM dispersion characterization; 3) numerical fate and transport modeling to derive delivered dose metrics (Figure 1). In more detail:

Part 1: ENM dispersion preparation—A reproducible dispersion preparation includes two key components:1) calorimetric calibration of the sonication equipment and reporting of

the delivered sonication energy (DSE) and duration in units of J/ml, and 2) determination of the material-specific critical sonication energy (DSE_{cr}) required to achieve a suspension with the smallest possible agglomerates that are minimally polydisperse and maximally stable over time. Importantly, sonication must be performed in water rather than culture media in order to avoid generation of reactive oxygen species by sonolysis and denaturing of proteins[33]. To generate dispersions in media for use in experiments, the material is first sonicated in deionized water with a delivered sonication energy (J/ml) greater than or equal to DSE_{cr}, and subsequently diluted in cell culture media to the desired initial concentration for application to cells (see Figure 2).

Part 2: ENM dispersion characterization—Characterization has become an increasing concern in ENM toxicological testing [33,61–66]. Robust characterization, including physical, chemical and morphological properties of ENM powders as well as colloidal properties of suspended ENMs, is essential for understanding biointeractions with cells. Lack of suitable ENM characterization, either of the pristine nanomaterials or of the dispersions, can call into question the validity and interpretability of *in vitro* toxicity data. Recent work by Warheit and Donner and others emphasizes the necessity of establishing and adopting standardized experimental procedures in order to make reliable toxicological determinations[53,67,68]. A summary of pristine ENM properties commonly evaluated is presented in Table 1. Here we will focus on the ENM suspension colloidal properties that drive particle transport in liquid suspension, and thus determine the dose delivered to cells *in vitro*, namely the size (diameter) and effective density of the formed agglomerates. In the protocol presented here we describe measurement of size distribution by dynamic light scattering (DLS), and measurement of effective density using volumetric centrifugation method (VCM).However, as discussed in more detail below, there are a variety of other instruments and methods available for accurately measuring size and effective density which can be used in place of the specific methods presented in this protocol.

Although analytical ultracentrifugation (AUC) is the gold standard for measurement of ENM effective density, it requires relatively expensive equipment not available in many labs, and is limited in terms of throughput. The VCM was developed by the authors to allow high-throughput measurement of effective density using a standard bench-top centrifuge, and relatively inexpensive packed cell volume (PCV) tubes[36]. Figure 3 presents a schematic overview of effective density measurement using the VCM. A known volume of suspension of a known ENM concentration is loaded into a PCV tube and centrifuged to collect the agglomerates in the capillary section of the tube. From the measured volume of the pellet and known volume of ENM, the effective density can be calculated as a weighted average of media and ENM.

Part 3: Fate and transport modeling for calculation of dose delivered to cells —With the stable suspension created and characterized, numerical modeling can then be used to compute the delivered dose metrics as a function of exposure time. The one dimensional model presented here, referred to as the distorted grid (DG) fate and transport model, provides both deposition and concentration metrics, and concentration profiles of ENMs across the well as a function of time [37]. The DG model also allows modeling of

variable binding kinetics at the bottom of the well, accommodates simultaneous simulation of polydisperse suspensions, and allows modeling of dissolution for soluble or partially soluble ENMs. The program is implemented in MATLAB, and typically runs in a few minutes before exporting dose metrics to an Excel file.

The entire integrated methodology, as well as its core components have previously been experimentally validated, as described in below in detail, for a variety of metal and metal oxide ENMs[36,37,54,55], and are suited for most low-aspect ratio nanomaterials.

Comparison with other methods

Several groups have recently proposed standardized dispersion protocols that result in reproducible and stable nanoparticle dispersions in media relevant for *in vitro* toxicity studies [33,69–73]. Review of these proposed standardized protocols highlights the key elements necessary for achieving and characterizing reproducible, stable, and relatively monodisperse suspensions for *in vitro* toxicity testing[68]. The protocol detailed here draws on best practices identified from those protocols, and achieves similar results in terms of agglomerate size, size distribution, and agglomerate stability over time[33].

In addition to DLS, the agglomerate size distribution can be measured using a variety of methods, including analytical ultracentrifugation (AUC), hydrodynamic chromatography, nanoparticle tracking analysis, laser diffraction spectrometry, x-ray disc centrifugation, and tunable resistive pulse sensing (TRPS)[38,54,74].Because DLS is easy to use and available in most nanotoxicology labs, and DLS output is suitable and has been validated for computational fate and transport modeling (see discussion of validation of computational modeling based on DLS measurements of size distribution below) [36,37,54,55], our protocol employs this method of size characterization. However, any of the other available methods for size characterization may be substituted for the DLS characterization presented here.

Measurement of effective density has presented a greater challenge. Despite its importance as a determinant of particle fate and transport, effective density is rarely characterized or reported for nanoparticle suspensions used in cellular toxicity studies[68]. This parameter can be empirically estimated based on a theoretical fractal-based model for agglomeration[75], or calculated from the sedimentation coefficient measured by analytical ultracentrifugation (AUC)[76]. Although AUC provides accurate direct measurement of effective density, the utility of this technique is hindered by the need for expensive laboratory equipment not often found in nanotoxicology labs, and by relatively low throughput. This protocol therefore provides detailed instructions for the recently developed VCM – an inexpensive, accessible, and high throughput method for measuring effective density. In previous publications we have validated VCM measurements of effective density against gold standard AUC measurements for a variety of both high and low density particles, as well as for the suitability of VCM measurements for validated computational modeling of particle fate and transport *in vitro* (see validation of computational modeling based on VCM measurements of effective density below)[36,37,54,55]. Nevertheless, AUC remains a gold standard for determination of effective density, and can be used in place of the VCM approach presented in this protocol.

The first computational model for estimating fate and transport of ENMs *in vitro* was the *In vitro* Sedimentation, Diffusion and Dosimetry model (ISDD), reported by Hinderliter et al. [77], which made it possible to calculate the per well bottom surface area deposited mass, surface area, and number of particles, as well as the fraction of total suspended material deposited as a function of time. This provided a ground-breaking improvement in dosimetry accuracy and enabled meaningful hazard rankings among ENMs to be obtained. The ISDD was subsequently adapted to utilize the VCM effective density, now referred to as VCM-ISDD[54]. The DG model developed by the authors and employed in the protocol presented here provides deposition as well as concentration metrics as a function of time, both at the bottom of the well and as a function of position in the well[37]. As mentioned above, the DG model also allows simultaneous simulation of all particles sizes in the distribution of a polydisperse suspension, and modeling of soluble materials. The DG model also allows modeling of variable binding kinetics ("stickiness") at the bottom of the well, based on a user-defined dissociation constant, K_D. As described in detail in our original report of the model, lower boundary binding kinetics can substantially affect delivered dose metrics[37]. Specifically, a perfectly sticky boundary, as employed by the ISDD model, can over-estimate the rate of particle settling, particularly for relatively small and light particles.

As described in detail in the original report, the integrated methodology presented here, including ENM dispersion preparation, characterization and dosimetry using the DG model, was validated by comparing predicted concentration profiles along the vertical axis for suspensions of metal oxide ENMs with empirical measurements of ENM concentration in thin cryosections from flash-frozen cylinders of ENM suspensions [37]. In addition, gold-standard three dimensional Computational Fluid Dynamics (CFD) models were developed and used to validate the DG model and the integrated methodology presented here. Very close agreement was observed between empirical cryosection measurements and both DG and CFD model predictions. The methodology had been further validated by our lab in terms of predicting biological outcome in an *in vitro* study of the hazard ranking of a large panel of low-aspect ratio ENMs[53].Details on the validation of this integrated *in vitro* dosimetry methodology can be found in papers previously published by the authors[33,36,37,53].

Experimental Design

Although the multi-step methodology described above is suitable for the majority of ENMs, in some circumstances it may be necessary to adapt the methodology to accommodate the specific characteristics of the ENM being used. ENMs that may require modification of the methodology include those that are significantly soluble, those that form particularly large agglomerates, and those that are buoyant.

The dissolution of ENMs over time can have important effects on properties of ENM dispersions and fate and transport modeling, and must be taken into account for significantly soluble materials (e.g. Ag, ZnO). For metal and metal oxide ENMs dissolution over time can be determined by employing one of several available techniques, including ultracentrifugation, either alone or combined with ultrafiltration[78,79], and dialysis[79–81], to remove undissolved particles, and subsequently quantifying the dissolved metal concentration in the resulting supernatants, ultrafiltrates or dialysates by IC-PMS. The

dissolved concentrations can then be used to determine the dissolved fraction and make the necessary adjustments to characterization and particle kinetics modeling and dose metrics, as described in detail below.

Some ENMs may also form large agglomerates containing very high amounts of media, such that the total agglomerate volume is large, and may block or overfill the PCV tube capillary. In these cases it may be necessary to repeat the protocol using a lower concentration, or to employ alternative methods such as AUC to estimate effective density. At the other extreme, ENMs that form small agglomerates may require longer than the 1 hour recommended (at 3000 × g) in this protocol to be completely pelleted. For example, given a VCM liquid column height of 3 cm, particles with a typical average effective density of 1.5 g/ml and diameter of 200 nm would require approximately 13 minutes to be pelleted, and those with diameter of 100 nm would require 50 minutes. However, particles with a diameter of 50 nm would require 198 minutes to pellet (~3.3 h). This time would be further increased for ENMs forming agglomerates with lower effective densities (sedimentation velocity is proportional to the difference between media density and ENM agglomerate effective density. Thus, when working with ENMs that form small and/or low density agglomerates, the centrifugation time for the VCM method may need to be increased substantially, and in some cases in which particles are smaller than ~50 nm, and/or have relatively low effective densities, it may be more efficient and practical to employ AUC to determine effective density.

Buoyant ENMs with density less than that of the media require adaptation of the VCM method, or use of an alternative method (e.g. AUC) for measurement of effective density. Because buoyant ENM agglomerates move toward rather than away from the rotor center during centrifugation, it is necessary to perform the VCM with the PCV tubes inverted in the centrifuge. Detailed methods for making these modifications and measuring effective density of buoyant particles are included in newly-published paper by the authors [46], and will not be presented here.

No specific controls are required for the dispersion preparation and determination of size by DLS, for effective density by the VCM method, or for subsequent dosimetry modeling. However, it is important that DLS instrumentation be regularly maintained, calibrated and validated according to manufacturers' guidelines. For example, standard particles of known size are available from DLS manufacturers, and should periodically be used to verify that the instrument is correctly measuring hydrodynamic diameters within the tolerance specified by the manufacturer.

Finally, the type of cell culture system and specific cells types used for *in vitro* testing depend upon the exposure type being emulated (e.g. inhalation, dermal, ingestion) and specific types of effects being investigated. For example, common immortal cell lines used for investigating possible effects of inhalation exposure include Human Small Airway Epithelial cells (SAECs), Human Microvascular Endothelial Cells (HMECs), and human THP-1 macrophages[26,55,60,82]. However, it is worth noting that the proposed methodology and protocols are independent of cell type and cellular assays.

Limitations

The proposed standardized methodology is limited to relatively low-aspect ratio ENMs. While this includes the vast majority of metal, metal oxide and many carbon-based ENMs, as well as incidental nanoparticles (*e.g.* resulting naturally *via* combustion processes), and particles released across the life cycle of nano-enabled products, this methodology is not suited to high-aspect ratio carbon nanotubes and other 2D ENMs such as graphene.This is due to the fact that: 1) dispersion of hydrophobic ENMs such as carbon nanotubes (CNTs) and graphene in aqueous media might be difficult using the approach described in part 1, since it often requires the use of specially-designed surfactants or other novel dispersants[83,84]; and 2) the sedimentation and diffusion equations underlying fate and transport modeling assume that particles or agglomerates can be approximated as spheres with a given hydrodynamic diameter. The hydrodynamic diameter, which is the product of the diameter of the sphere of equivalent volume and a frictional coefficient that accounts for non-spherical shape and surface irregularity, is used to calculate both sedimentation and diffusion coefficients needed to model transport. Hydrodynamic diameter can be measured directly by methods such as DLS, and can often be estimated for non-spherical shapes when only the equivalent diameter is known. For prolate or oblate ellipsoids, or rigid rods, for example, it is possible to approximate frictional coefficients in order to arrive at hydrodynamic diameters and enable fate and transport modeling using the DG model. However for very long rods (non-agglomerated carbon nanotubes), or non-rigid, or branching structures (e.g. nanofibrillar cellulose) the situation is more complex and fate and transport modeling approaches have as yet not been worked out. In such cases it may be possible to employ an empirical method, such as flash freezing columns of suspension at various time points, cryosectioning those frozen columns, and applying various methods to quantify the content of nanomaterial in each section. Investigations into the internalized particle dose *via* mass spectrometry[85], or tracking cellular uptake of fluorescent- or radiolabeled particles [55] may provide alternative approaches for estimating dosimetry in these cases. Similarly, the ENM suspension preparation protocols described here may not be suitable for generating relatively monodisperse suspensions for such high-aspect ratio and hydrophobic ENMs. More research is needed to determine suitable methods for preparing and characterizing suspensions and performing dosimetry analysis for such ENMs

Materials

Reagents

- Sterile deionized water
- Cell culture media of choice (*for example,* RPMI 1640, ThermoFisher Scientific, cat. no. 11875093, or DMEM, ThermoFisher Scientific, cat. no. 11995065,supplemented with 10% (vol/vol) fetal bovine serum [FBS], ThermoFisher Scientific, cat. no. 16000044)
- ENMs: The methodology described can be successfully applied to all low-aspect ratio ENMs, including metal and metal oxide ENMs obtained from commercial vendors (for example Sigma Aldrich Fe_2O_3 , cat. no 544884, and TiO_2 , cat. no 637262), or produced industrially or in the lab by methods such as Flame Spray

Pyrolysis (for example, as generated by the Harvard Versatile Engineered Nanomaterial Generation System (VENGES)[86] as described previously[42,86,87], or generated during use or disposal of nano-enabled products and ambient nanoparticles collected from air samples[25,88].

Equipment

- High precision laboratory scale or analytical balance (for example, Mettler Toledo XPE205DR, cat. no. 30087700)
- Sonicator (for example, Branson S-450D, 400 W, Branson, part. no. 101-063-590) CRITICAL a minimum power rating of 250 W is recommended to allow reasonable sonication times, and may be necessary to achieve adequate dispersion
- Sonicator cup horn (for example, Branson 3-inch I.D., Flow through, Branson, part. no. 101-147-048)
- Small 3-prong dual adjust clamp (*e.g.* Southern Labware SKU: 916056)
- Flexible PVC tubing for connecting water source to cup horn inlet and cup horn outlets to drain. For the Branson 3-inch I.D. cup horn, a tubing with inside diameter of 3/8 inch is required (for example, VWR Signature™ Clear PVC Tubing, I.D. 3/8 inch, 50 ft., cat. no. 60985-540)
- Sound enclosure for sonicator set up (for example, Branson, part no. 101-063-275)
- 15 ml and 50 ml conical polypropylene or polystyrene centrifuge tubes (for example, Falcon, part. no. 352097 (15 ml) and 352070 (50 ml))
- Laboratory vortex mixer (for example, VWR, cat. no. 97043-562)
- Dynamic Light Scattering instrument (for example, Zetasizer Nanoseries Nano ZS, Malvern) or any other colloidal nanoparticle size characterization instrument
- TPP Packed Cell Volume (PCV) tubes without graduations (TPP Techno Plastic Products AG, part no. 87005) and caps (TPP Techno Plastic Products AG, part no. 87008)
- Easy read measuring device for PCV tubes (TPP Techno Plastic Products AG, part no. 87010)
- Laboratory centrifuge (for example, Beckman Coulter Allegra 6, part no. 366802)
- Swinging bucket rotor (for example, Beckman Coulter GH-3.8A, part no. 366650) CRITICAL Rotor must be swinging bucket style, NOT fixed angle.
- Microtube size bucket adapter (for example, Beckman Coulter, part no. 359469)
- Viscometer with a range of ≤0.5 to ≥2.0 cSt (for example, size 25 Cannon-Fenske tube viscometer, Sigma-Aldrich, cat. no. Z275263)

- PC running Windows 7 or 10, minimum 4 GB RAM.
- MATLAB core product for Windows, version 2013a or later. No toolboxes are required.
- Microsoft Excel 2010 or later.
- DG model .m file: DG_nanotransport_simulator.m (provided as Supplementary Software “DG_nanotransport_simulator.m”).

Equipment Setup

Sonicator setup—The following instructions describe the general setup of the Branson S-450 D Sonifier with Branson 3-inch up horn. Consult the product manual for detailed instructions for this and any other devices. Connect the sonicator cup horn the converter, and the converter to the power supply (*i.e.* the Branson S-450D). Secure the cup horn within the acoustic enclosure. Connect the cup horn coolant inlet port to a cold water source, and outlet and overflow ports to a drain using 0.25” plastic tubing (for the Branson 3-inch cup horn). Adjust the 3-pronged clamp to hold conical centrifuge tubes in the center of the cup horn.

Procedure

Part 1: ENM Dispersion Preparation TIMING 2.5 – 5 hrs

CRITICAL As described in Equipment Setup, the sonicator must be calibrated calorimetrically prior use to ensure that the exact delivered sonication energy is known and reported for any experiment. This will also ensure that sonicators from different manufacturers or models can be used to deliver the specific sonication energy of interest.

1 | *Sonicator Calorimetric Calibration to obtain Delivered Sonication Energy (DSE) rate (DSE/m) (1-2 hrs):* Drill a hole large enough for the thermometer probe (a suitable hole can be created with a box cutter) in the cap of a 50 ml conical centrifuge tube.

2 | Add 50 ml deionized water to the 50 ml conical centrifuge tube.

3 | Insert thermometer probe through the hole and into the water in the tube.

4 | Turn the thermometer on.

5 | Position and secure the tube in a three-pronged clamp in the center of the cup horn.

6 | Turn sonicator power on, select and record power settings (for example, 75% amplitude, continuous mode)

7 | Turn on the cup horn water source and adjust flow so that the sample meniscus is aligned with the water level in the cup.

9 | Turn the sonicator power on.

10 | Record temperature every 10-30 seconds until the temperature stabilizes (~3-5 minutes), and turn the sonicator power off.

?Troubleshooting

11 | Repeat Steps 2-10 two times to generate a total of three data sets.

12 | Calculate the delivered acoustic power P (W = J/s) as

$$P = \left({}^{dT}/_{dt} \right) \mathrm{MC}_p,$$

where ${}^{dT}/_{dt}$ is the slope of temperature (K) vs. time (s), M is the mass of water (5 g for 5 ml deionized water), and C_p is the specific heat of water (4.186 J/g°K)

13 | Calculate and record the average power, P (J/s), from the three measurements (for the specific sonicator and sonicator settings used).

14 | *Determination of Critical Delivered Sonication Energy (DSE_{cr}) (1-2 hrs):* Weigh approximately 1 mg of nanoparticle powder into a 15 ml conical centrifuge tube.

15 | Add deionized water to achieve a final concentration of 0.5 mg/ml.

16 | Vortex suspension at high speed for 30 seconds.

17 | Remove 1 ml of the suspension, measure the mean hydrodynamic diameter using DLS or other size characterization instrumentation, and return the sample to the tube.

18 | Adjust sonicator power settings to those used during calibration (step 6) and turn the sonicator power on.

19 | Sonicate the particle suspension for one to two minutes.

20| Calculate delivered sonication energy (DSE, J/ml) for the sonication step as

$$\mathrm{DSE} = P \times t / V,$$

where P is the delivered acoustic power determined in the calibration steps 1 to 13, t is time in seconds, and V is the volume of the suspension in ml.

21 | Remove 1 ml of the suspension, measure the mean hydrodynamic diameter using DLS or other size characterization instrumentation, and return the sample to the tube.

22 | Repeat steps 19-21 until the mean hydrodynamic diameter decreases by <5% between steps.

23 | Plot cumulative DSE (x axis) vs. mean hydrodynamic diameter (y axis).

24 | Identify the $\mathrm{DSE}_{\mathrm{cr}}$ (J/ml) as the cumulative DSE at which further sonication does not further reduce the mean hydrodynamic diameter by more than 5% (slope approaches zero).

25 | Remove a 100 μl sample of suspension, dilute to 100 μg/ml in culture media of choice, and measure mean hydrodynamic diameter of the sample by DLS or other size characterization instrumentation.

26 | Repeat size measurement of suspension in culture media at 24 hours.

CRITICAL STEP If mean size changes substantially (by more than 30%) at 24 hours, it may be advisable to repeat Steps 14-26 with additional sonication time until the 24 hours post-sonication suspension mean size is more consistent with that at time 0. DSE_{cr} refers to the energy per unit volume of suspension required to achieve smallest possible agglomerates, *and* most stable suspensions over time. Although some change in size over time due to re-agglomeration is not uncommon, large deviations in mean size indicate an unstable suspension, suggesting that additional power is needed to completely disrupt the forces between primary particles.

27 | *Preparation of suspensions for characterization and use in experiments (30 min – 1 hr):*Weigh the amount of nanoparticle powder required for the experiment into a 15 ml conical centrifuge tube.

28 | Add deionized water to achieve a final concentration of 0.5 mg/ml.

CRITICAL Maximum volume for sonication in a typical 3” cup horn is approximately 5 ml. It may not be possible to effectively deliver energy to suspensions of greater volume. If larger amounts of suspension are required, split them into portions of less than or equal to 5 ml each.

29 | Vortex suspension at high speed for 30 seconds.

30 | Select sonicator power settings and turn sonicator power on.

CRITICAL Use the same power settings used to calibrate sonicator and to measure DSE_{cr}.

31 | Calculate time t (s) required for sonication as

$$t = V \times {}^{\mathrm{DSE_{cr}}}/_{P},$$

where V is the volume of suspension (ml), and P is the delivered power (W or J/s) determined by calibration (Steps 1-13).

32 | Sonicate the suspension for the calculated time required.

33 | Vortex suspension at high speed for 30 seconds

34 | Dilute to the final desired concentrations in media or fluid of choice for characterization or experimental studies.

Part 2: ENM Dispersion Characterization TIMING 3 - 5 hrs

CRITICAL Note that effective density can alternatively be measured by analytical ultracentrifugation (AUC).

35 | *Determination of suspended nanomaterial effective density (ρ_{EV}) (2-4 hrs):*Dilute water suspension prepared as described above into desired media to make ~4 ml of suspension at 100 μg/ml.

36 | Transfer 1 ml of suspension into each of three PCV tubes and cap the tubes.

37 | Centrifuge tubes at room temperature for 1 hour at 3000 × *g*.

38 | Use the “Easy read” measuring device to measure the volume of the pellet collected at the bottom of the capillary in each PCV tubes.

?Troubleshooting—CRITICAL STEP: It is important to use the easy read device correctly to avoid errors. The device resembles a thick ruler. The front face is etched along the top with graduations at 0.025 µl intervals. Insert the PCV tube into hole on top of the sliding holder so that it rests on the ramp at the back of the ruler. The holder contains a lens to magnify the capillary and ruler graduations. Slide the tube and holder along the ramp until the top edge of the pellet is aligned with the top. Position your line of sight so that the horizontal cross-hair is aligned with the top edge of the ruler, and the vertical line of the cross hair is aligned with the capillary center. If not properly aligned parallax error will result in measurement error. (see Figure 3 b).

?Troubleshooting

39 | Calculate density of media, ρ_{media} (g/cm^3) by weighing a known volume of media in a tared vessel, or by subtracting the mass of a pre-weighed vessel from the mass of the vessel with the media, and dividing by the volume.

40 | Calculate the effective density, ρ_{EV}, for each measured pellet volume using the following equation:

$$\rho_{\mathrm{EV}} = \rho_{\mathrm{media}} + \left[\left(\frac{M_{\mathrm{ENM}} - M_{\mathrm{ENMsol}}}{V_{\mathrm{pellet}} \mathrm{SF}} \right) \left(1 - \frac{\rho_{\mathrm{media}}}{\rho_{\mathrm{ENM}}} \right) \right],$$

Where ρ_{media} is the density of the media (g/cm^3), M_{ENM} is the total mass of nanomaterial (g) in the dispensed volume (1 ml) of suspension (e.g., 1.0 ml × 100 µg/ml × 1×10^{-6} g/µg = 1.0 × 10^{-4} g) is the mass of dissolved nanomaterial (g) in the dispensed volume (1 ml) of suspension. For insoluble materials M_{ENMsol} is 0. For soluble materials M_{ENMsol} must be determined by analyzing the supernatant (e.g. by ICP-MS) of an ENM suspension after centrifugation. Dissolution measurements are beyond the scope of this paper but suitable methods can be found in numerous sources in the literature[78–81]. From the concentration of dissolved ENM, the mass of dissolved ENM can be calculated (e.g., 1.0 ml × 10 µg/ml × 1 × 10^{-6} g/µg = 1.0 × 10^{-5} g), is the measured pellet size in cm^3 (convert measured volume, which is in µl or mm^3, to cm^3 by dividing by 1000), ρ_{ENM} is the density (g/cm^3) of the raw nanomaterial (e.g. 5.242 g/cm^3 for Fe_2O_3). SF is the stacking factor, which is the portion of the pellet that is composed of agglomerates (the remaining portion being inter-agglomerate media). Values for SF may range from 0.634 for random stacking, to the theoretical maximum of 0.74 for ordered stacking[89,90]. For the roughly spherical agglomerates typically observed with low-aspect ratio ENMs we have verified that the theoretical value for random close stacking (0.634) is appropriate, whereas for uniform non-agglomerating spherical ENMs (e.g. gold spheres), the theoretical value for ordered stacking (0.74) should be used[36].

41 | Calculate the mean ρ_{EV} from the three individual measures.

42 | *Determination of Size (hydrodynamic diameter) distribution (1-2 hrs):*Power on Zetasizer Nanoseries 30 minutes before use.

CRITICAL STEP: The following steps describe size characterization using a Zetasizer Nanoseries DLS instrument. For other DLS instruments refer to the manufacturer's instructions. As discussed in the introduction, several other types of instrumentation for measuring colloidal size distribution are available and can be used in place of DLS.

43 | Turn on accompanying PC or laptop computer and open Zetasizer software.

44 | Transfer 1.0 ml of sample to a Malvern disposable cuvette.

45 | Insert cuvette into DLS machine and close cover

46 | Select material-media specific SOP (Standard Operating Procedure, which contains material- and media- specific properties needed by the instrument) if one exists, and if no SOP exists for specific material and media, create a new SOP by entering the material-specific refractive index and absorption and the media-specific viscosity.

47 | Run SOP to collect the mean hydrodynamic diameter and the intensity-, number- and volume-weighted size distributions.

CRITICAL STEP: The three types of distribution obtained from DLS (intensity-, number- and volume-weighed) often differ somewhat from one another. Specifically, the intensity-weighted distribution can be relatively skewed toward larger sizes, whereas the number distribution can be skewed toward larger smaller sizes. For calculation of DSE_{cr} described above (Steps 14-26), the mean hydrodynamic diameter reported by the instrument is used. For fate and transport modeling, described below, the most accurate results are obtained using the volume-weighted distribution, which best represents the mass distribution of the suspended material.

?Troubleshooting

Part 3: Fate and transport modeling for calculation of dose delivered to cells TIMING 30 mins - 1 hrs

48 | *Analysis of Particle Kinetics and Calculating Dose metrics with Fate and Transport modeling (Distorted Grid model) (30 mins - 1 h):* Open the .m file DG_nanotransport_simulator.m in the MATLAB editor.

49 | Enter the solvent/media properties. Each user input data parameter is listed as uid. *name*, where *name* is a descriptive name of the parameter. “uid.” is a MATLAB data structure of which all of the named parameters are elements. This is followed by the assignment operator “=”, a number value, and a closing semicolon; For each parameter, change the associated number value (or values in the case of arrays) to the appropriate data for your experimental system. The solvent/media properties to be entered are the solvent viscosity (uid.solvent_viscosity) in Pa s (See Box 1), the solvent density (uid.solvent_density) in g/cm^3, and the temperature of the system (uid.solvent_temperature) in degrees Celsius.

50 | Enter particle properties. These include the ENM raw material density (uid.material_density) in g/cm^3, the particle diameters for each particle size species present (uid.particle_diameters) in nm, the volume-weighted fraction of the total volume of ENM corresponding to the particle diameters (uid.species_fractions), and the agglomerate or particle effective density (uid.particle_effective_density), in g/cm^3. The particle diameters and corresponding species fractions are arrays, enclosed by square brackets. It is possible to enter single average particle size, in which case the corresponding species fraction array would contain the single value of 1.0. However, more accurate results can be obtained if the particle size distribution and corresponding fractions (e.g., the volume-weighted size distribution obtained by DLS) are used.

51 | Enter experimental parameters. These include the height of the liquid column within the cell culture well (uid.column_height) in mm (e.g., 3.0 mm for a typical 96-well plate with 100 ul suspension per well), the initial concentration of ENM (uid.initial_concentration) in mg/cm^3, and the total simulation time (uid.simulation_time) in hours. The simulation time should be set to the duration of the *in vitro* exposure incubation.

52 | Enter model parameters. These define the resolution in space and time, of the simulation, and usually do not need to be changed from their default values. The model divides the height of the well into a number of small compartments, and performs alternating short rounds of sedimentation and diffusion between these compartments. The compartment height (uid.compartment_height) specifies the height of these small compartments in mm. It is usually set to 0.005, and should not require changing, unless a finer resolution of the vertical concentration profile is desired. The duration of the short rounds of sedimentation and diffusion is specified by the simulation time interval (uid.simulation_time_interval), in seconds. The default is 0.5 seconds. Larger values (1.0 – 2.0 seconds) may reduce the time for the simulation to run, however this will also reduce the accuracy of the results.

53 | Enter output data parameters. These specify the temporal and spatial resolution of the dosimetry output data, and options that may save time if only some of the output is required. The output time interval (uid.output_time_interval), in minutes, specifies the time between saved data points. The output compartment height (uid.output_compartment_height), in mm, is the vertical resolution of the output concentration profile. It is also the height of the bottom compartment that defines the thickness of the cell microenvironment. Deposition metrics are calculated based on the amount of material in this compartment.

54 | Enter dissolution parameters. If the ENM being analyzed is soluble, and dissolution data has been obtained, it can be entered here. The initial dissolution fraction (uid.initial_dissolution) is the fraction of ENM dissolved at the start of the incubation. The dissolution rate type (uid.dissolution_rate_type) defines the type of dissolution data that will be provided. If no further dilution occurs after initial dissolution, then the dissolution rate type should be set to 0. If dissolution occurs at a constant rate (constant fraction of ENM dissolves per unit time) then the dissolution

rate type should be set to 1. If dissolution is not linear, and measurements were made at multiple time points, then the dissolution rate type should be set to 2. The dissolution rate (uid.dissolution_rate) is only relevant when the dissolution rate type is set to 1, and specifies the fraction of the total ENM that dissolves per hour. The last two dissolution parameters, dissolution times (uid.dissolution_times) and dissolution fractions (uid.dissolution_fractions) are relevant if the dissolution rate type is set to 2, and specify the time points and dissolved fractions in the dissolution curve.

55 | Enter Particle-cell adsorption parameters. These parameters are used to control whether and with what affinity particles are adsorbed to the cell surfaces at the bottom of the well. The uid.sticky parameter determines whether adsorption occurs (set to 1) or not (set to 0). If set to 0, then the value of the second adsorption parameter, the dissociation constant (uid.adsorption_dissociation_constant), in units of Molarity, is ignored and irrelevant, and the bottom boundary condition for the simulation is perfectly reflective. If uid.sticky is set to 1, then the degree of stickiness is determined by the dissociation constant. Typically, significant effects on transport (dose metrics) only occur for dissociation constant values less than about 1×10^{-9} M.

56 | Save changes and execute the .m file. While the simulation is running the percentage completed will be displayed in the MATLAB command window.

57 | Export results to an excel file. When the simulation is complete a prompt will appear for providing a name and location for the output Excel file. This file contains dose metrics over the course of the simulation time. See Box 2 for a description of the file format.

Troubleshooting

Advice for troubleshooting potential problems is provided in Table 3.

Timing

Part 1: ENM Dispersion Preparation, 2.5–5 hrs

Steps 1-13, Calibration of Sonicator, 1-2 hr

Steps 14-26, Determination of DSE_{cr}, 1-2 hr

Steps 27-34, Preparation of suspensions for experiments, 30 mins to 1 hr

Part 2:ENM Dispersion Characterization, 3-5 hrs

Steps 35-41, Determination of effective density, 2-4 hrs

Steps 42-47, Determination of size distribution by DLS, 1 hr

Part 3: Fate and transport modeling for calculation of dose delivered to cells, 30 mins - 1 hr

Steps 48-57, Particle kinetics and dosimetry, 30 m - 1 hr

Anticipated Results

The step-by-step protocol detailed above can be used to determine *in vitro* dose metrics for most low-aspect ratio ENMs, including engineered nanomaterials, incidental nanoparticles (*e.g.* resulting naturally *via* combustion processes), and nano-sized particles released across the life cycle of nano-enabled products.

To illustrate the use of this protocol with a typical ENM, we provide here highlights for a case study using a common metal oxide ENM (Fe_2O_3) to determine dose metrics in a 96-well plate over 24 hours. The Fe_2O_3 material for this case study was made by Flame Spray Pyrolysis (FPS) using the Harvard Versatile Engineered Nanomaterial Generation System (VENGES)[86]as described previously[42,86,87].The powder characterization and colloidal characterization in DMEM + 10% (vol/vol) FBS for this material are presented in Table 4. The sonicator used was a Branson model S-450D with 3-inch I.D. cup horn, which was calibrated using Steps 1-13 and determined to deliver a power 2.59 J/s.

Determination of Critical Delivered Sonication Energy (DSE_{cr})

DSE_{cr} for the Fe_2O_3 material was determined following Steps 14-26.Mean hydrodynamic diameter (obtained by DLS) is shown plotted as a function of applied energy in Figure 4. From this graph we determined that DSE_{cr} for the material is 345 J/ml. The mean hydrodynamic diameter in media immediately after dilution was determined by DLS to be 976 nm. At 24 hours after dispersion in media the mean hydrodynamic diameter was found by DLS to be 717 nm, suggesting that the formed agglomerates were not perfectly stable. Since the difference was within 30% this change was deemed acceptable. It is possible in some cases sonication in water for a longer time (selecting a higher DSE_{cr}) will further improve stability of the suspension in media. For this material, sonication at a higher DSE did not significantly improve stability of the media suspension (data not shown).

Colloidal characterization of the ENM suspension:effective density and size distribution

The effective density (ρ_{EV}) for the Fe_2O_3 ENM in DMEM + 10% (vol/vol) FBS was measured using the VCM method according to Steps 35-41. The density of the media, total and dissolved mass of ENM, raw ENM density and stacking factor used in the calculation of effective density were as follows:

$\rho_{media} = 1.0084\ g/cm^3$

$M_{ENM} = 1.0\ ml \times 100\ \mu g/ml \times 1x10^{-6}\ g/\mu g = 1.0 \times 10^{-4}\ g$

$M_{ENMsol} = 0.0\ g$ (insoluble material)

$\rho_{ENM} = 5.242\ g/cm^3$ (Fe_2O_3)

$SF = 0.634$

The three measured pellet volumes and calculated effective densities were as shown in Table 5. The mean effective density from these three measurements was $1.483\ g/cm^3$.

The size distribution of the suspension was measured by DLS (Steps 42-47) and is represented in Figure 5.

Analysis of Particle Kinetics and Calculating Dose metrics with Fate and Transport modeling

The effective density and volume weighted size distribution determined above were used to determine dose using the DG model. In the MATLAB file 'DG_nanotransport_simulator.m' (Supplementary Software), the list of sizes and corresponding volume-weighted fractions (from DLS), and effective density have been assigned to the relevant variables, and all other variables have been set as described above in Steps 49-55. The simulation was then run, and data exported to the file 'DG_output_Fe2O3_CaseStudy.xlsx' (Supplementary Data). The output metrics described above in Box 2 and Table 2 can be found in this file. As described in Box 2, all metrics at the bottom of the well are presented in the 'Bot Summary' tab, and there are additional tabs for each metric that provide each metric as a function of both time and vertical position in the well. The mean for each metric has been calculated and added to the Bot Summary tab. The fraction deposited and mass concentration vs. time plots automatically generated by the program are shown in Figure 6. From these plots it is clear that the agglomerates sediment relatively quickly to reach a maximum equilibrium concentration at the bottom of the well (24.8 mg/ml) and fraction deposited (0.82) at approximately 11 hours. The mean concentration at the bottom of the well (22.7 mg/ml) and mean fraction deposited (0.76) over the simulated exposure time are also presented in the output graphs in Figure 6.

Supplementary Material

Refer to Web version on PubMed Central for supplementary material.

Acknowledgments

This research project was supported by Harvard-NIEHS Nanosafety Center grant (1U24ES026946) and NSF grant 1436450.

References

1. Ma X, Wang Q, Rossi L, Ebbs SD, White JC. Multigenerational exposure to cerium oxide nanoparticles: Physiological and biochemical analysis reveals transmissible changes in rapid cycling Brassica rapa. NanoImpact. 2016; 1:46–54.
2. Pyrgiotakis G, et al. A chemical free, nanotechnology-based method for airborne bacterial inactivation using engineered water nanostructures. Environ Sci Nano. 2014; 1:15–26.
3. Pyrgiotakis G, et al. Mycobacteria inactivation using Engineered Water Nanostructures (EWNS). Nanomedicine. 2014; 10:1175–83. [PubMed: 24632246]
4. Pyrgiotakis G, et al. Inactivation of foodborne microorganisms using engineered water nanostructures (EWNS). Environ Sci Technol. 2015; 49:3737–45. [PubMed: 25695127]
5. Pyrgiotakis G, et al. Optimization of a nanotechnology based antimicrobial platform for food safety applications using Engineered Water Nanostructures (EWNS). Sci Rep. 2016; 6:21073. [PubMed: 26875817]
6. Roco, MC., Mirkin, CA., Hersan, MC. Nanotechnology Research Directions for Societal Needs in 2020, Retrospective and Outlook. Springer; 2011.

7. Servin AD, White JC. Nanotechnology in agriculture: Next steps for understanding engineered nanoparticle exposure and risk. NanoImpact. 2016; 1:9–12.
8. Sotiriou GA, et al. Engineering safer-by-design, transparent, silica-coated ZnO nanorods with reduced DNA damage potential. Environ Sci Nano. 2014; 1:144–153. [PubMed: 24955241]
9. Bott J, Störmer A, Franz R. A model study into the migration potential of nanoparticles from plastics nanocomposites for food contact. Food Packag Shelf Life. 2014; 2:73–80.
10. Froggett SJ, Clancy SF, Boverhof DR, Canady RA. A review and perspective of existing research on the release of nanomaterials from solid nanocomposites. Part Fibre Toxicol. 2014; 11:17. [PubMed: 24708765]
11. Grassian VH, et al. NanoEHS – defining fundamental science needs: no easy feat when the simple itself is complex. Environ Sci Nano. 2016; 3:15–27.
12. Konduru NV, et al. Silica coating influences the corona and biokinetics of cerium oxide nanoparticles. Part Fibre Toxicol. 2015; 12:31. [PubMed: 26458946]
13. Lu X, et al. In vivo epigenetic effects induced by engineered nanomaterials: A case study of copper oxide and laser printer-emitted engineered nanoparticles. Nanotoxicology. 2016; 10:629–39. [PubMed: 26559097]
14. Pal AK, et al. Linking Exposures of Particles Released From Nano-Enabled Products to Toxicology: An Integrated Methodology for Particle Sampling, Extraction, Dispersion, and Dosing. Toxicol Sci. 2015; 146:321–33. [PubMed: 25997654]
15. Watson C, et al. High-throughput screening platform for engineered nanoparticle-mediated genotoxicity using CometChip technology. ACS Nano. 2014; 8:2118–33. [PubMed: 24617523]
16. Yetisen AK, et al. Nanotechnology in Textiles. ACS Nano. 2016; 10:3042–3068. [PubMed: 26918485]
17. Zhou EH, et al. Assessing the impact of engineered nanoparticles on wound healing using a novel in vitro bioassay. Nanomedicine (Lond). 2014; 9:2803–15. [PubMed: 24823434]
18. Balbus JM, et al. Meeting report: hazard assessment for nanoparticles--report from an interdisciplinary workshop. Environ Health Perspect. 2007; 115:1654–9. [PubMed: 18007999]
19. George S, et al. Use of a high-throughput screening approach coupled with in vivo zebrafish embryo screening to develop hazard ranking for engineered nanomaterials. ACS Nano. 2011; 5:1805–17. [PubMed: 21323332]
20. Krewski D, et al. Toxicity testing in the 21st century: a vision and a strategy. J Toxicol Environ Health B Crit Rev. 2010; 13:51–138. [PubMed: 20574894]
21. Lai DY. Toward toxicity testing of nanomaterials in the 21st century: a paradigm for moving forward. Wiley Interdiscip Rev Nanomed Nanobiotechnol. 4:1–15. [PubMed: 21965171]
22. Warheit DB, Borm PJA, Hennes C, Lademann J. Testing strategies to establish the safety of nanomaterials: conclusions of an ECETOC workshop. Inhal Toxicol. 2007; 19:631–43. [PubMed: 17510836]
23. Keller AA, McFerran S, Lazareva A, Suh S. Global life cycle releases of engineered nanomaterials. J Nanoparticle Res. 2013; 15:1692.
24. Wigger H, et al. Influences of use activities and waste management on environmental releases of engineered nanomaterials. Sci Total Environ. 2015; 535:160–71. [PubMed: 25728395]
25. Pirela SV, et al. Development and characterization of an exposure platform suitable for physico-chemical, morphological and toxicological characterization of printer-emitted particles (PEPs). Inhal Toxicol. 2014; 26:400–8. [PubMed: 24862974]
26. Sisler JD, et al. Small airway epithelial cells exposure to printer-emitted engineered nanoparticles induces cellular effects on human microvascular endothelial cells in an alveolar-capillary co-culture model. Nanotoxicology. 2015; 9:769–79. [PubMed: 25387250]
27. Sotiriou GA, et al. An integrated methodology for the assessment of environmental health implications during thermal decomposition of nano-enabled products. Environ Sci Nano. 2015; 2:262–272. [PubMed: 26200119]
28. Wohlleben W, et al. On the lifecycle of nanocomposites: comparing released fragments and their in-vivo hazards from three release mechanisms and four nanocomposites. Small. 2011; 7:2384–95. [PubMed: 21671434]

29. Pirela SV, et al. Effects of intratracheally instilled laser printer-emitted engineered nanoparticles in a mouse model: A case study of toxicological implications from nanomaterials released during consumer use. NanoImpact. 2016; 1:1–8. [PubMed: 26989787]
30. Pirela SV, et al. Consumer exposures to laser printer-emitted engineered nanoparticles: A case study of life-cycle implications from nano-enabled products. Nanotoxicology. 2015; 9:760–8. [PubMed: 25387251]
31. Pirela S, et al. Effects of copy center particles on the lungs: a toxicological characterization using a Balb/c mouse model. Inhal Toxicol. 2013; 25:498–508. [PubMed: 23895351]
32. Demokritou P, et al. An in vivo and in vitro toxicological characterisation of realistic nanoscale CeO_2 inhalation exposures. Nanotoxicology. 2013; 7:1338–50. [PubMed: 23061914]
33. Cohen J, Deloid G, Pyrgiotakis G, Demokritou P. Interactions of engineered nanomaterials in physiological media and implications for in vitro dosimetry. Nanotoxicology. 2013; 7:417–31. [PubMed: 22393878]
34. Gangwal S, et al. Informing selection of nanomaterial concentrations for ToxCast in vitro testing based on occupational exposure potential. Environ Health Perspect. 2011; 119:1539–46. [PubMed: 21788197]
35. Oberdörster G. Nanotoxicology: in vitro-in vivo dosimetry. Environ Health Perspect. 2012; 120:A13. author reply A13. [PubMed: 22214547]
36. DeLoid G, et al. Estimating the effective density of engineered nanomaterials for in vitro dosimetry. Nat Commun. 2014; 5:3514. [PubMed: 24675174]
37. DeLoid GM, et al. Advanced computational modeling for in vitro nanomaterial dosimetry. Part Fibre Toxicol. 2015; 12:32. [PubMed: 26497802]
38. Pal AK, et al. High resolution characterization of engineered nanomaterial dispersions in complex media using tunable resistive pulse sensing technology. ACS Nano. 2014; 8:9003–15. [PubMed: 25093451]
39. Teeguarden JG, Hinderliter PM, Orr G, Thrall BD, Pounds JG. Particokinetics in vitro: dosimetry considerations for in vitro nanoparticle toxicity assessments. Toxicol Sci. 2007; 95:300–12. [PubMed: 17098817]
40. Bakand S, Winder C, Khalil C, Hayes A. Toxicity assessment of industrial chemicals and airborne contaminants: transition from in vivo to in vitro test methods: a review. Inhal Toxicol. 2005; 17:775–87. [PubMed: 16195213]
41. Pyrgiotakis G, Blattmann CO, Demokritou P. Real-Time Nanoparticle-Cell Interactions in Physiological Media by Atomic Force Microscopy. ACS Sustain Chem Eng. 2014; 2:1681–1690. [PubMed: 25068097]
42. Pyrgiotakis G, Blattmann CO, Pratsinis S, Demokritou P. Nanoparticle-nanoparticle interactions in biological media by atomic force microscopy. Langmuir. 2013; 29:11385–95. [PubMed: 23978039]
43. Lundqvist M, et al. The evolution of the protein corona around nanoparticles: a test study. ACS Nano. 2011; 5:7503–9. [PubMed: 21861491]
44. Buford MC, Hamilton RF, Holian A. A comparison of dispersing media for various engineered carbon nanoparticles. Part Fibre Toxicol. 2007; 4:6. [PubMed: 17655771]
45. Sharma G, et al. Iron oxide nanoparticle agglomeration influences dose rates and modulates oxidative stress-mediated dose-response profiles in vitro. Nanotoxicology. 2014; 8:663–75. [PubMed: 23837572]
46. Watson CY, DeLoid GM, Pal A, Demokritou P. Buoyant Nanoparticles: Implications for Nano-Biointeractions in Cellular Studies. Small. 2016; 12:3172–3180. [PubMed: 27135209]
47. Cai, W Bin, et al. The Optimized Fabrication of Nanobubbles as Ultrasound Contrast Agents for Tumor Imaging. Sci Rep. 2015; 5:13725. [PubMed: 26333917]
48. DasSarma S, et al. An improved genetic system for bioengineering buoyant gas vesicle nanoparticles from Haloarchaea. BMC Biotechnol. 2013; 13:112. [PubMed: 24359319]
49. Schmit VL, Martoglio R, Scott B, Strickland AD, Carron KT. Lab-on-a-bubble: synthesis, characterization, and evaluation of buoyant gold nanoparticle-coated silica spheres. J Am Chem Soc. 2012; 134:59–62. [PubMed: 22077992]

50. Suzuki R, Maruyama K. Effective in vitro and in vivo gene delivery by the combination of liposomal bubbles (bubble liposomes) and ultrasound exposure. Methods Mol Biol. 2010; 605:473–86. [PubMed: 20072902]
51. Wittmaack K. Excessive Delivery of Nanostructured Matter to Submersed Cells Caused by Rapid Gravitational Settling. ACS Nano. 2011; 5:3766–3778. [PubMed: 21446668]
52. Wittmaack K. Novel Dose Metric for Apparent Cytotoxicity Effects Generated by in Vitro Cell Exposure to Silica Nanoparticles. Chem Res Toxicol. 2011; 24:150–158. [PubMed: 21171596]
53. Pal AK, Bello D, Cohen J, Demokritou P. Implications of in vitro dosimetry on toxicological ranking of low aspect ratio engineered nanomaterials. Nanotoxicology. 2015; :1–15. DOI: 10.3109/17435390.2014.986670
54. Cohen JM, Teeguarden JG, Demokritou P. An integrated approach for the in vitro dosimetry of engineered nanomaterials. Part Fibre Toxicol. 2014; 11:20. [PubMed: 24885440]
55. Cohen JM, et al. Tracking translocation of industrially relevant engineered nanomaterials (ENMs) across alveolar epithelial monolayers in vitro. Nanotoxicology. 2014; 8(Suppl 1):216–25. [PubMed: 24479615]
56. Kreyling WG, et al. In vitro and in vivo interactions of selected nanoparticles with rodent serum proteins and their consequences in biokinetics. Beilstein J Nanotechnol. 2014; 5:1699–711. [PubMed: 25383281]
57. Anjilvel S, Asgharian B. A multiple-path model of particle deposition in the rat lung. Fundam Appl Toxicol. 1995; 28:41–50. [PubMed: 8566482]
58. Cassee FR, et al. Particle size-dependent total mass deposition in lungs determines inhalation toxicity of cadmium chloride aerosols in rats. Application of a multiple path dosimetry model. Arch Toxicol. 2002; 76:277–86. [PubMed: 12107645]
59. Geraets L, Oomen AG, Schroeter JD, Coleman VA, Cassee FR. Tissue distribution of inhaled micro- and nano-sized cerium oxide particles in rats: results from a 28-day exposure study. Toxicol Sci. 2012; 127:463–73. [PubMed: 22430073]
60. Pirela SV, et al. Effects of Laser Printer-Emitted Engineered Nanoparticles on Cytotoxicity, Chemokine Expression, Reactive Oxygen Species, DNA Methylation, and DNA Damage: A Comprehensive in Vitro Analysis in Human Small Airway Epithelial Cells, Macrophages, and Lymphobla. Environ Health Perspect. 2015; doi: 10.1289/ehp.1409582
61. Powers KW, Palazuelos M, Moudgil BM, Roberts SM. Characterization of the size, shape, and state of dispersion of nanoparticles for toxicological studies. Nanotoxicology. 2007; 1:42–51.
62. Powers KW, et al. Research strategies for safety evaluation of nanomaterials. Part VI. Characterization of nanoscale particles for toxicological evaluation. Toxicol Sci. 2006; 90:296–303. [PubMed: 16407094]
63. Brown SC, et al. Nanoparticle characterization for cancer nanotechnology and other biological applications. Methods Mol Biol. 2010; 624:39–65. [PubMed: 20217588]
64. Brown SC, et al. Influence of shape, adhesion and simulated lung mechanics on amorphous silica nanoparticle toxicity. Adv Powder Technol. 2007; 18:69–79.
65. Crist RM, et al. Common pitfalls in nanotechnology: lessons learned from NCI's Nanotechnology Characterization Laboratory. Integr Biol (Camb). 2013; 5:66–73. [PubMed: 22772974]
66. Patri A, et al. Nanotechnology characterization laboratory: A resource for translational research in nanomedicine. Abstr Pap Am Chem S 2008. 2008; 236
67. Warheit DB, Donner EM. How meaningful are risk determinations in the absence of a complete dataset? Making the case for publishing standardized test guideline and ‘no effect’ studies for evaluating the safety of nanoparticulates versus spurious ‘high effect’ results from single. Sci Technol Adv Mater. 2015; 16
68. Cohen JM, DeLoid GM, Demokritou P. A critical review of in vitro dosimetry for engineered nanomaterials. Nanomedicine (Lond). 2015; doi: 10.2217/nnm.15.129
69. Schulze C, et al. Not ready to use – overcoming pitfalls when dispersing nanoparticles in physiological media. Nanotoxicology. 2008; 2:51–61.
70. Taurozzi JS, Hackley VA, Weisner MW. Preparation of Nanoparticle Dispersions from Powdered Material Using Ultrasonic Disruption. 2012; doi: 10.6028/NIST.SP.1200-2

71. Taurozzi JS, Hackley VA, Wiesner MR. Ultrasonic dispersion of nanoparticles for environmental, health and safety assessment--issues and recommendations. Nanotoxicology. 2011; 5:711–29. [PubMed: 21073401]
72. Taurozzi JS, Hackley VA, Wiesner MR. A standardised approach for the dispersion of titanium dioxide nanoparticles in biological media. Nanotoxicology. 2013; 7:389–401. [PubMed: 22397515]
73. Wu W, et al. Dispersion method for safety research on manufactured nanomaterials. Ind Health. 2014; 52:54–65. [PubMed: 24305513]
74. Wohlleben W. Validity range of centrifuges for the regulation of nanomaterials: from classification to as-tested coronas. J Nanopart Res. 2012; 14:1300. [PubMed: 23239934]
75. Sterling MC, Bonner JS, Ernest ANS, Page CA, Autenrieth RL. Application of fractal flocculation and vertical transport model to aquatic sol-sediment systems. Water Res. 2005; 39:1818–30. [PubMed: 15899280]
76. Carney RP, et al. Determination of nanoparticle size distribution together with density or molecular weight by 2D analytical ultracentrifugation. Nat Commun. 2011; 2:335. [PubMed: 21654635]
77. Hinderliter PM, et al. ISDD: A computational model of particle sedimentation, diffusion and target cell dosimetry for in vitro toxicity studies. Part Fibre Toxicol. 2010; 7:36. [PubMed: 21118529]
78. Ma R, et al. Size-controlled dissolution of organic-coated silver nanoparticles. Environ Sci Technol. 2012; 46:752–9. [PubMed: 22142034]
79. Odzak N, Kistler D, Behra R, Sigg L. Dissolution of metal and metal oxide nanoparticles in aqueous media. Environ Pollut. 2014; 191:132–8. [PubMed: 24832924]
80. Kittler S, Greulich C, Diendorf J, Köller M, Epple M. Toxicity of Silver Nanoparticles Increases during Storage Because of Slow Dissolution under Release of Silver Ions. Chem Mater. 2010; 22:4548–4554.
81. Vasyukova E, Pokrovsky OS, Viers J, Dupré B. New operational method of testing colloid complexation with metals in natural waters. Appl Geochemistry. 2012; 27:1226–1237.
82. Lu X, et al. Short-term exposure to engineered nanomaterials affects cellular epigenome. Nanotoxicology. 2015; :1–11. DOI: 10.3109/17435390.2015.1025115
83. Ayán-Varela M, et al. Achieving extremely concentrated aqueous dispersions of graphene flakes and catalytically efficient graphene-metal nanoparticle hybrids with flavin mononucleotide as a high-performance stabilizer. ACS Appl Mater Interfaces. 2015; 7:10293–307. [PubMed: 25915172]
84. Zhang L, et al. Rationally designed surfactants for few-layered graphene exfoliation: ionic groups attached to electron-deficient π-conjugated unit through alkyl spacers. ACS Nano. 2014; 8:6663–70. [PubMed: 24968119]
85. Vanhecke D, et al. Quantification of nanoparticles at the single-cell level: an overview about state-of-the-art techniques and their limitations. Nanomedicine (Lond). 2014; 9:1885–900. [PubMed: 25325243]
86. Demokritou P, et al. Development and characterization of a Versatile Engineered Nanomaterial Generation System (VENGES) suitable for toxicological studies. Inhal Toxicol. 2010; 22 Suppl 2:107–16. [PubMed: 20701428]
87. Gass S, et al. A Safer Formulation Concept for Flame-Generated Engineered Nanomaterials. ACS Sustain Chem Eng. 2013; 1:843–857. [PubMed: 23961338]
88. Sotiriou GA, et al. Thermal decomposition of nano-enabled thermoplastics: Possible environmental health and safety implications. J Hazard Mater. 2016; 305:87–95. [PubMed: 26642449]
89. Gauss CF. Besprechung des Buchs von L.A. Seeber: Untersuchungen über die Eigenschaften der positiven ternären quadratischen Formen usw. Göttingsche Gelehrt Anzeigen. 1831; 2:188–196.
90. Song C, Wang P, Makse HA. A phase diagram for jammed matter. Nature. 2008; 453:629–632. [PubMed: 18509438]

Box 1

Determination of media dynamic viscosity

Because particle transport rates, both diffusion and sedimentation, are inversely proportional to media dynamic viscosity, it is important to accurately measure this property before proceeding to fate and transport modeling. Because viscosity is temperature dependent, it is important that it be measured at the temperature at which the ENM suspensions will be incubated with cells (e.g. 37° C). For example, at room temperature (22° C) the dynamic viscosity of RPMI culture media supplemented with 10% (vol/vol) heat-inactivated Fetal bovine serum is, by our measurements, 0.00103 pascal-seconds (Pa s), whereas at 37° C the viscosity of the same media is 0.00081 Pa s (22% lower).

A number of options are available for measurement of viscosity, including inexpensive glass U-tube (Ostwald or Cannon-Fenske) viscometers, somewhat more expensive falling ball viscometers, more expensive rotational viscometers, and others. When selecting a viscometer be sure that it is capable of measuring in the 0.5 to 2.0 centistokes (cSt) range. The viscosity of water at 22° C is 1.0 cSt, and most biological fluids and culture media have viscosities of between 0.75 and 1.25 cSt.

Methods for proper use of a viscometer are provided by the manufacturers and will not be presented here. Most viscometers yield the kinematic viscosity v, in the cgs unit cSt. Use the following formula to convert to dynamic viscosity, η, in SI units (pascal-seconds, Pa s), which is the value required for fate and transport modeling inputs (utilized within the code for calculation of diffusion and sedimentation coefficients):

$$\eta(\mathrm{Pa\,s}) = v(\mathrm{cSt}) \times \rho \times 10^{-3}$$

where ρ is the density of the media in kg/m3 (equivalent to g/cm3).

Box 2

Analysis of DG model output data

The Excel output file generated by the DG model contains several relevant dose metrics at each output time point (defined by the chosen parameters uid.simulation_time and uid.output_time_interval) during the simulated time. These metrics are summarized in Table 2, and include mass, particle number, and surface area concentrations per unit volume as well as per unit well bottom area, and fraction of administered ENM deposited (within the bottom compartment). For materials that are soluble, the concentration of dissolved material is also provided, and mass concentrations are provided both including and excluding the dissolved material contribution. In addition, if the simulation includes adsorption (uid.sticky set to 1), the mass bound per unit area and the percentage of the bottom occupied by adsorbed particles are provided.

The output Excel file contains multiple sheets. In the sheet named ‘Bot Summary’, the dose metrics in Table 2 are given for each time point at the bottom of the well, (i.e., within the bottom compartment, representing the cell microenvironment, the height of which is defined by the parameter uid.output_compartment_height selected for the simulation - typically 0.01 mm or 10 μm). In addition to the Bottom Summary sheet, the DG output file contains one sheet for each of the above parameters, in which the value of that parameter over time is given at the center z position of each compartment (defined by uid.output_compartment_height selected when running the simulation).

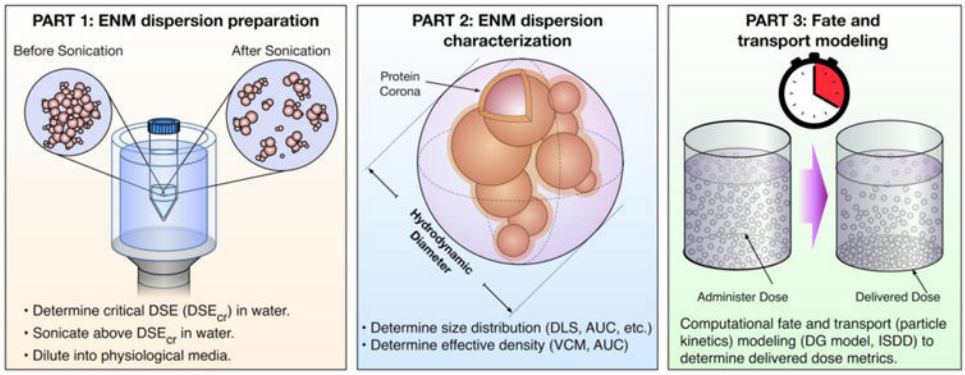

Figure 1. Harvard Dispersion Dosimetry Protocol (HDDP)

A hybrid experimental and computational approach to determine accurate dosimetry for *in vitro* toxicology study. The methodology includes 3 major parts illustrated here: ENM dispersion preparation, characterization of the ENM dispersion (hydrodynamic diameter and effective density), and computational fate and transport modeling to determine dosimetry.

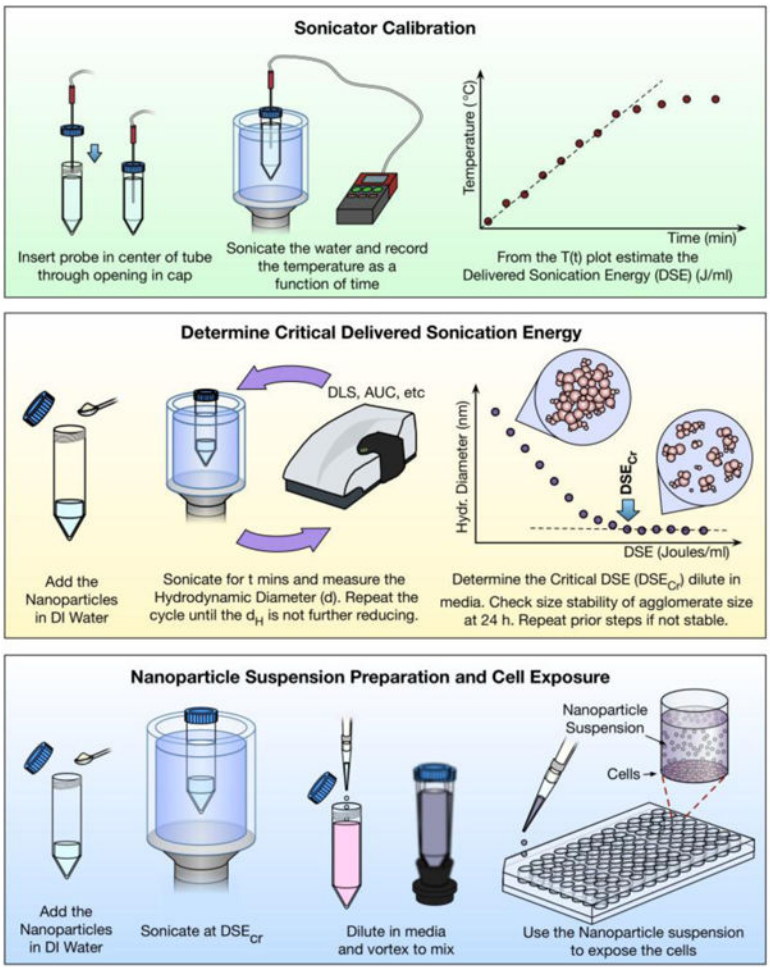

Figure 2. ENM Dispersion Protocol

Key steps in preparation of ENM dispersions include initial calibration of sonication equipment to determine delivered sonication energy, and determination of the critical sonication energy (DSE_{cr}) required to produce the smallest and most stable dispersion of the specific ENM. Preparation of ENM suspensions for application to cultured cells in in vitro experiments is then performed by sonicating in water above DSE_{cr} and diluting to the desired concentration in culture media.

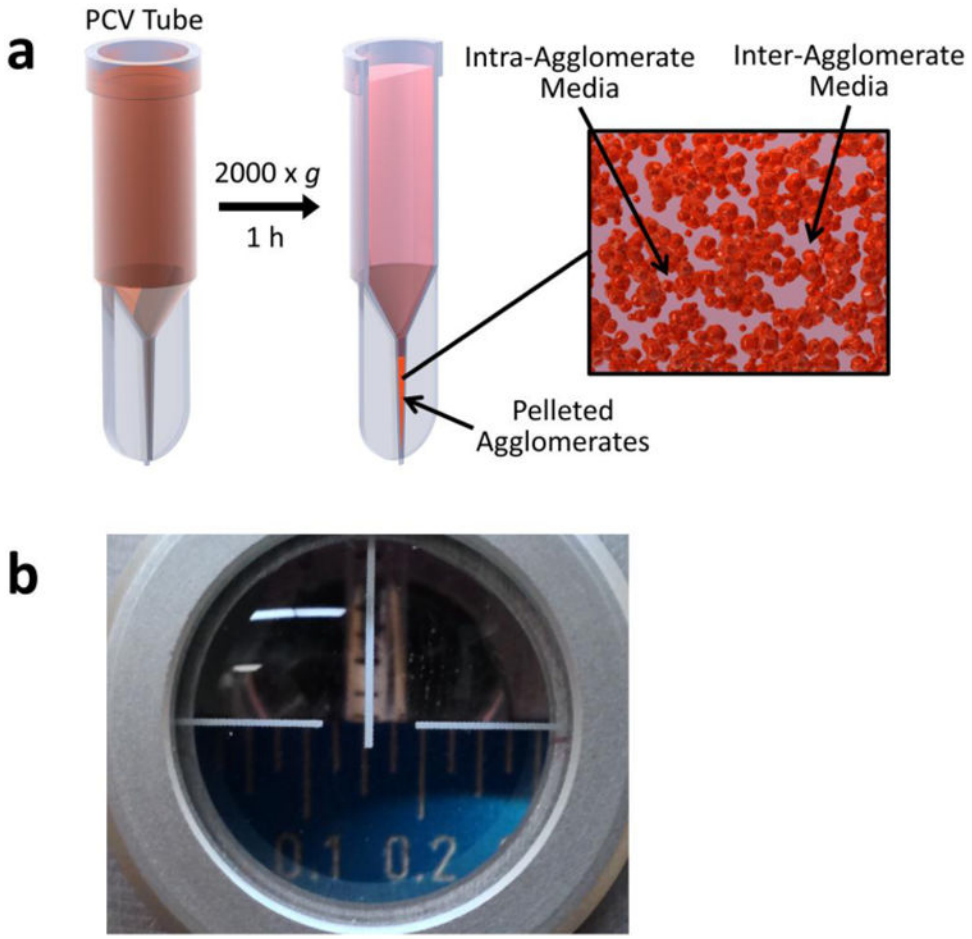

Figure 3. Volumetric Centrifugation Method (VCM)

a, Packed cell volume (PCV) tube (adapted with permission from DeLoid et al., 2014[36]). **b**, Measurement of the pellet volume with the slide-rule like easy-read device. Image shows a pellet volume reading of 0.15 μL

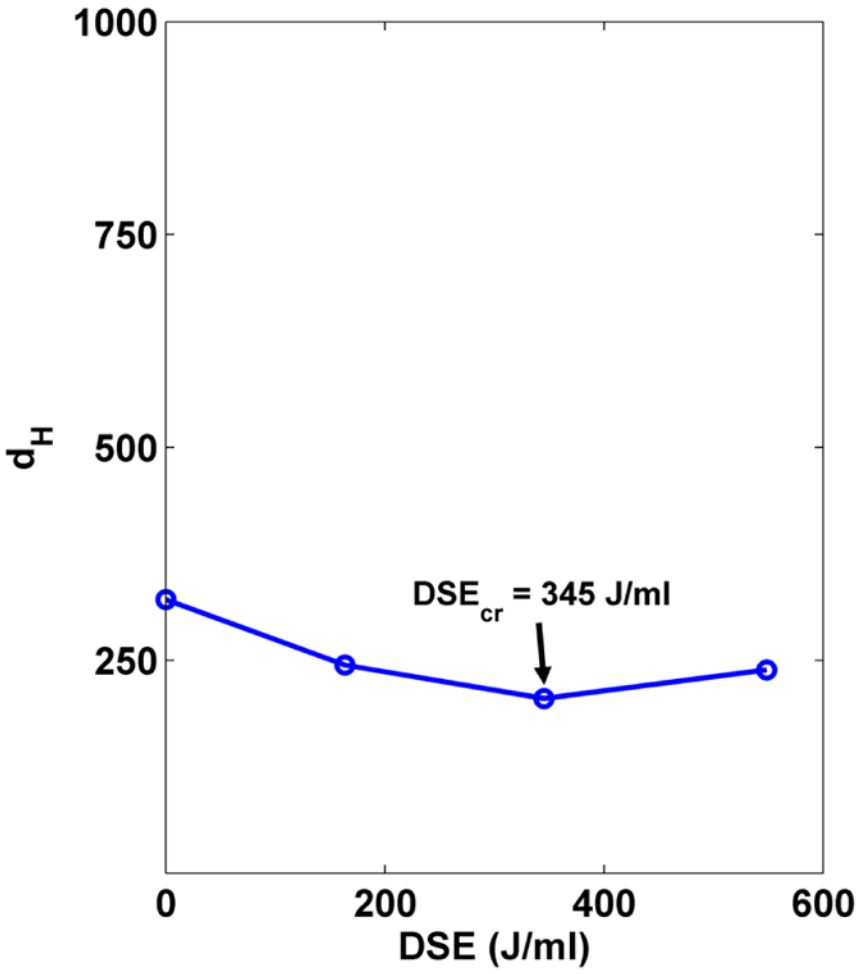

Figure 4. Determining DSE

$_{cr}$. Mean hydrodynamic diameter as a function of Dispersion Sonication Energy.

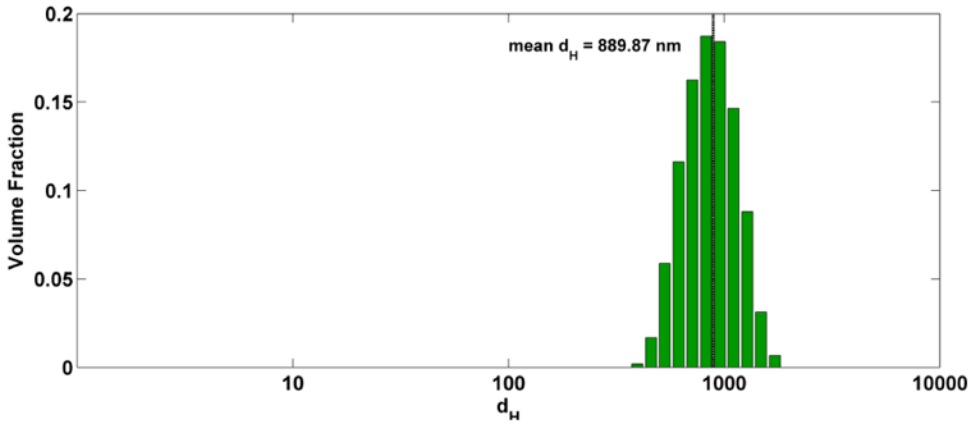

Figure 5. Volume size distribution

Size (volume-weighted hydrodynamic diameter) distribution of dispersions in cell culture media.

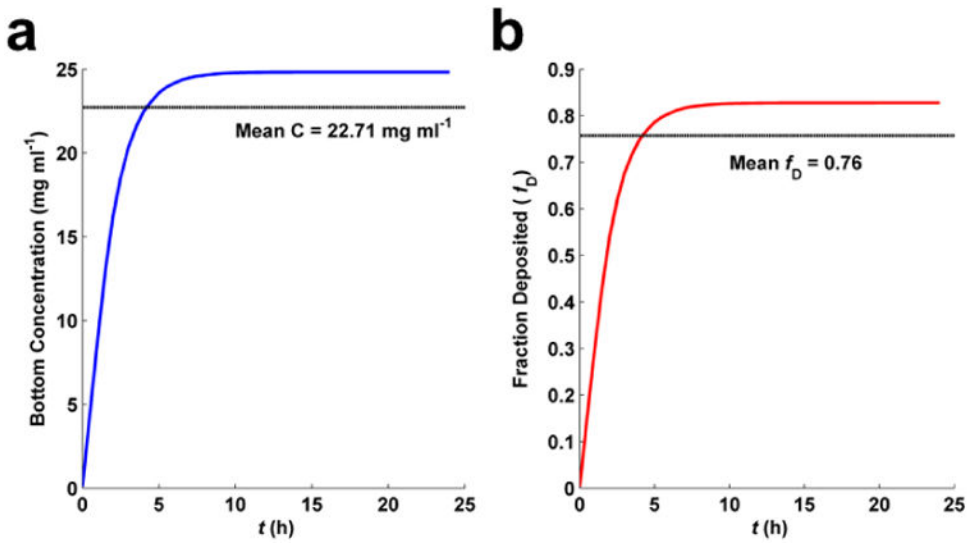

Figure 6. Fate and Transport modeling results

a, Well bottom ENM (Fe_2O_3) concentration over time of simulation.. **b**, Fraction of ENM deposited over time of simulation.

Table 1
ENM properties relevant for *in vitro* nanotoxicology

Properties		Methods	Notes
Physical & Morphological	Density	Pycnometer	Relevant for attributing particle properties to biological repsonses
	Surface area	BET[1]	
	Porosity	BET/alkaline Homologous Series	
	Surface Roughness	BET/ Anvir and Pfiefer Method	
	Charge	Faraday Pail Device	
	Crystal Structure*	XRD[2], TEM-SAD[3]	
	Size	XRD-Rietveld analysis, BET, TEM	
	Shape, Aspect ratio	TEM-Image analysis	
	Size distribution	TEM-Image analysis	
Chemical	Composition	ICP-MS[4], TEM-EDS[5], TGA[6], EC-OC[7], Raman spectroscopy (carbon ENMs), FTIR[8] (cellulose)	
	Surface chemistry.	FTIR, XPS[9]	
	Molecular Weight	ICP-MS (metals and oxides), weight analysis (oxides)	
	Hydrophobicity/philicity	Dye ads.; Octanol-water affinity	
Colloidal	**Size distribution**	**DLS[10], TRPS[11], DC[12],TEM**	**Relevant for *in vitro* dosimetry**
	Polydispersity	**DLS, TRPS**	
	Effective density	**VCM[15], AUC[16]**	
	Dissolution	**ICP-MS**	
	pH	pH meter	Relevant for particle-media interactions and biological responses
	Corona	DLS, ELS, LC-MS/MS[14]	
	Specific conductance	DLS	
	Zeta potential	ELS[13], TRPS	

[1] Brunauer–Emmett–Teller;

[2] X-Ray Diffractions;

[3] TEM-Selected Area Diffraction;

[4] Inductive Coupled Plasma Mass Spectroscopy,

[5] Transmission Electron Microscopy-Electron Dispersive Spectroscopy;

[6] Thermo-Gravitational Analysis;

[7] Elemental Carbon-Organic Carbon;

[8] Fourier Transform Infrared Spectroscopy;

[9] X-Ray Photoelectron Spectroscopy;

[10] Dynamic Light Scattering;

[11] Tunable resistive pulse sensing;

[12] Electrophoresis Light scattering;

[13] Disc Centrifugation,

[14] Liquid Chromatography Tandem Mass Spectrometry;

[15] Volume Centrifugation Method;

[16] Analytical Ultracentrifugation

Table 2

DG model Excel output dose metrics

Parameter	Units	Meaning
Mp vol^{-1}	mg cm^{-3}	mass of ENM per unit volume, not including dissolved ENM
Mp+DissC vol^{-1}	mg cm^{-3}	mass of ENM per unit volume, including dissolved ENM
Frx Mp	N/A	Fraction of administered ENM deposited (within compartment, e.g. bottom compartment, cell microenvironment)
Mp $area^{-1}$	mg cm^{-2}	mass of ENM per unit area of well bottom, not including dissolved ENM
Mp+DissC $area^{-1}$	mg cm^{-2}	mass of ENM per unit area of well bottom, including dissolved ENM
Np vol^{-1}	cm^{-3}	number of particles per unit volume
Np $area^{-2}$	cm^{-2}	number of particles per unit area of well bottom
SAp vol^{-1}	cm^2 cm^{-3}	ENM surface area per unit volume
SAp $area^{-1}$	cm^2 cm^{-2}	ENM surface area per unit area of well bottom
DissC vol^{-1}	mg cm^{-3}	mass of dissolved ENM per unit volume
% floor occ.	%	percent of well bottom occupied by adsorbed particles (only reported for uid.sticky = 1)
Mbound $area^{-1}$	mg cm^{-2}	mass of ENM bound to bottom per area of well bottom (only reported for uid.sticky = 1)

Table 3

Troubleshooting table

Step	Problem	Possible Reason	Solution
Calibration of Sonicator Step 10	Water temperature rises quickly and levels off providing limited data points for calibration curve	Low volume of water sample can absorb a limited amount of energy before reaching thermal equilibrium, at which point temperature will stop rising.	For calorimetric calibration use at least 50 ml of water.
Measuring VCM pellet size Step 38	Cannot see pellet	1. Insufficient material in suspension to form a visible pellet.	Repeat VCM (Steps 35-38) with a higher concentration of material.
		2. Small particles (<100 nm) may not reach bottom of capillary in 1 hour.	Increase centrifugation time. If no pellet after 4 hours, consider using AUC.
		3. ENM may be buoyant (density < media density)	Refer to Watson et al. [46] for possible adaptation of VCM method, or use AUC to measure effective density.
	Pellet clogs top of capillary or over-fills capillary of VCM tube	1. Total volume of agglomerates may be too large	Repeat VCM (Steps 35-38) with a lower concentration of material.
		2. Agglomerates are too large to enter capillary tube	VCM cannot be used. Use an alternative method, such as AUC, to determine effective density
	Pellet is lodged on the side of the VCM tube	Centrifuge bucket was not horizontal during centrifugation (e.g. a fixed angle rotor was used)	Repeat VCM using a swinging bucket rotor.
Measuring particle size (DLS) Step 47	Multimodal size distribution	Dispersion not sonicated sufficiently	Prepare fresh solution with dispersion sonicated to the material-specific critical delivered sonication energy (DSE_{cr})

Table 4

Fe_2O_3 ENM characterization

ENM powder properties			Colloidal properties in DMEM + 10% (vol/vol) heat-inactivated FBS				
SSA (m^2/g)	**d_{BET} (nm)**	**d_{XRD} (nm)**	**d_H (nm)**	**PdI**	**ζ (mV)**	**σ (mS/cm)**	**ρ_{EV}**
54.7	20.9	27.2	976.0	0.40	-14.4	13.8	1.483

SSA: specific surface area measured by nitrogen adsorption by the Brunauer-Emmet-Teller (BET) method, d_{BET}: primary particle diameter determined from SSA. d_{XRD}: particle diameter measured by X-ray diffraction, d_H: hydrodynamic diameter measured by DLS, PdI: polydispersity index, ζ: zeta potential, σ: specific conductance, ρ_{EV}: effective density measured by VCM.

Table 5

Calculation of effective density

V_{pellet} (cm^3)	$\rho_{EV}=\rho_{media}+\left[\left(\frac{M_{ENM}-M_{ENMsol}}{V_{pellet}SF}\right)\left(1-\frac{\rho_{media}}{\rho_{ENM}}\right)\right]$ (g/cm^3)
2.75×10^{-4}	1.427
3.0×10^{-4}	1.433
2.375×10^{-4}	1.545